Computers and Concrete, Vol. 10, No. 1 (2012) 59-78
DOI: http://dx.doi.org/10.12989/cac.2012.10.1.059

Analysis of RC beam with unbonded or exposed tensile steel reinforcements and defective stirrup anchorages for shear strength

Xiao-Hui Wang* and Xi-La Liu

Department of Civil Engineering, Shanghai Jiaotong University, Shanghai, 200240, P.R. China

(Received August 18, 2010, Revised April 30, 2011, Accepted November 18, 2011)

Abstract. Although the effect of corrosion of reinforcing bar on the shear behavior of the reinforced concrete (RC) beam had been simulated by tests of the beam with unbonded, half-exposed or whole-exposed tensile steel reinforcements as well as defective stirrup anchorages, theoretical methods to accurately predict remaining capacity of this kind of RC beams, especially shear capacity, are still lacking. Considering the possible position of the critical inclined crack, the actual pattern of strains in the concrete body within the partial length and the proposed compatibility condition of deformations of the RC beam, shear strength of the RC beam with unbonded or exposed tensile steel reinforcements and/or defective stirrup anchorages is predicted. Comparison between the model's predictions with the experimental results published in the literature shows the practicability of the proposed model. Influence of the length of unbonded or exposed tensile steel reinforcements and the percentage of stirrups lacked end anchorages on the shear strength of the RC beam is discussed. It is concluded that, the shear strength of the RC beam with unbonded or exposed tensile steel reinforcements and/or defective stirrup anchorages is greatly influenced by the length of unbonded or exposed tensile steel reinforcements and the percentage of stirrups lacked end anchorages, this influence can be adverse, insignificant or even favourable, dependent on the given parameters of the corresponding normal bonded RC beam.

Keywords: shear strength; unbonded length; critical inclined crack; defective stirrup anchorages.

1. Introduction

The problem of the deterioration of safety-related reinforced concrete (RC) structures due to corrosion of the steel reinforcement has received worldwide attention since it has been identified as one of the most predominant factors for the degradation of the RC structures. Due to the need to understand the effects of deterioration on the residual load bearing capacity of deteriorated RC elements and enhance the currently used inspection procedures to plan strategic and cost-effective rehabilitation methods, a lot of research works have been carried out to study the performance and residual strength of corrosion-damaged RC elements. Considering the actual corrosion condition in existing RC elements, where corrosion of the reinforcing bars in the RC elements may occur only within a partial length of the RC elements, such as in the areas close to the supports and in the central part of the RC beam (Castel *et al.* 2000, Vidal *et al.* 2007), experimental works on the mechanical behavior and load capacity of RC structural elements with partially corrosion-damaged

* Corresponding author, Ph.D., E-mail: w_xiaoh@163.com

length were carried out (Toogoenthong and Maekawa 2004a, 2004b, Torres-Acosta *et al.* 2004, EI Maaddawy *et al.* 2005, Higgins and Farrow III 2006, Du *et al.* 2007, Wang and Liang 2008, Malumbela *et al.* 2009, Azam 2010, Suffern *et al.* 2010, Wang *et al.* 2011).

About the shear behaviour of the RC beam with partially unbonded length, most research works are experimental (Cairns 1995, Kim and White 1999, Jeppsson and Thelandersson 2003, Yu 2005, Regan and Kennedy Reid 2004). In order to experimentally simulate the effect of corrosion of reinforcing bar on the behavior of the RC beam, the tensile steel reinforcements was unbonded, half-exposed or whole-exposed within a fraction of the beam length and/or certain percentage stirrups lacked end anchorages (Cairns 1995, Kim and White 1999, Jeppsson and Thelandersson 2003, Regan and Kennedy Reid 2004, Yu 2005). Among those experimental works, Cairns (1995) presented three test series A~C to study the shear behavior of the concrete beams with exposed reinforcements. The test results indicated that the exposure of bars was found to increase the strength of the beam designed to fail in shear, in some cases by a substantial margin. Kim and White (1999) described an experimental investigation into the cause of critical-shear cracking in slender RC beams, including six series of specimens. The effect of unbonded tension reinforcement on shear crack pattern and load-carrying capacity was studied in UBB series beams. It is concluded that the elimination of bond resulted in a drastic change in failure mode as well as a large increase in load capacity. Jeppsson and Thelandersson (2003) presented experimental investigation on the behavior and reduction of shear capacity for concrete beams with loss of bond for the longitudinal reinforcement close to a support. It was found that, in spite of significant loss of bond, only a moderate reduction in load carrying capacity was observed, implying that short bond lengths are sufficient to create high bond forces. Even if the failure mechanism is still shear, the failure did not become more brittle as could be expected. Regan and Kennedy Reid (2004) described the results of tests of beams with varying proportions of the stirrups lacked end anchorages and half-exposed tensile steel. It was found that, the shear strength of the beam was reduced by the stirrups without end anchorages and the exposed lower main bars; however, this loss of strength was limited. Yu (2005) presented RC beams with exposed tensile steel in different zones along the beam length.

Due to the complex of the shear resistance mechanism of the noncorroded RC beam, it becomes more difficult in predicting the shear capacity of the corrosion-damaged RC beam. Till now, only Cairns (1995) proposed a method of analysis to evaluate the shear strength of beams with a part of the longitudinal reinforcement exposed over varying portions of the span on the basis of the existing semi-empirical rules in BS 8110. The analysis suggested that shear strength was increased when reinforcement was exposed in all but the most lightly reinforced section. For the RC beam with varying proportions of the stirrups lacked end anchorages and half-exposed tensile steel, a modified truss model incorporating defective stirrups was proposed (Regan and Kennedy Reid 2004).

In the present paper, considering the possible position of the critical inclined crack, the actual pattern of strains in the concrete body within the partial length and the proposed compatibility condition of deformations of the RC beam, shear strength of the RC beam with unbonded or exposed tensile steel reinforcements and/or defective stirrup anchorages is predicted. The practicability of the proposed models is shown via the comparison between the model's predictions with the experimental results published in the literature. Then, influence of the length of unbonded or exposed tensile steel reinforcements and the percentage of stirrups lacked end anchorages on the shear strength of the RC beam is discussed and some conclusions are obtained.

2. Material modeling

2.1 Concrete

The stress-strain relationship of concrete in compression is defined as a parabolic relationship (Collins and Mitchell 1987), is given by

$$\sigma_c = f_c' \cdot [2\varepsilon_c / \varepsilon_0 - (\varepsilon_c / \varepsilon_0)^2] \tag{1}$$

where ε_0 is taken as $\varepsilon_0 = 0.002$; f_c' is the cylinder compressive strength of concrete.

2.2 Steel reinforcement

The stress-strain relationship of steel reinforcement is idealized to be elastic perfectly plastic, and can be expressed as follows

$$\sigma_s = \begin{cases} E_s \varepsilon_s & \varepsilon_s \le \varepsilon_y \\ f_y & \varepsilon_s > \varepsilon_y \end{cases} \tag{2}$$

where ε_y is the yield strain of steel reinforcement, $\varepsilon_y = f_y / E_s$; E_s is the modulus of steel reinforcement; f_y is the yield strength of steel reinforcement.

3. Shear strength modeling of the RC beam with unbonded or exposed tensile steel reinforcements and/or defective stirrup anchorages

In this paper, RC beam with partially length L_{ub} symmetrically arranged about the mid-span of the beam is considered (see Fig. 1), where the distance between the support and the extra edge of the partial length is $a_A = a_v + L_0/2 - L_{ub}/2$. For the beam shown in Fig. 1(b), due to the whole tensile steel within L_{ub} is exposed, the bond strength between the steel and concrete is also complete lost. Thus, for beams shown in Figs. 1(a) and (b), the same methodology can be used to predict the shear strength of the beams. According to the test results of Kim and White (1999), the critical inclined crack can not form due to the existence of the unbonded length within the shear span, avoiding the typical shear failure. In predicting the shear strength of the beam with unbonded steel within L_{ub}, the possible formation position of the critical inclined crack need to be considered and the scheme of the shear failure is described in Figs. 1(a) and (b). However, for the beam shown in Fig. 1(c), the half-exposed lower tensile steel within the whole beam span and even the 67% of stirrups lacked end anchorages results in no signs of breakdown of bond (Regan and Kennedy Reid 2004). So, the formation position of the critical inclined crack is little influenced.

At a location a_{cr}, a tensile crack develops and the tensile strain of the concrete reaches $\varepsilon_{cr} = f_r / E_c$, where f_r is the modulus of rupture of concrete, $f_r = 0.625\sqrt{f_c'}$, f_c' is the cylinder strength of concrete. With an additional applied force $0.05\sqrt{f_c'} \cdot bh_0^{pub}$ (MPa), this tensile crack can reach the neutral axis of the beam (Park *et al*. 2006, Choi *et al.* 2007). Then, for the RC beam with partial length in Fig. 1, the moment M_{cr} at a_{cr} is given as

$$M_{cr} = M_{cr}' + 0.05\sqrt{f_c'} \cdot b \cdot h_0^{pub} \cdot a_{cr} \tag{3}$$

where b is the beam width; h_0^{pub} is the effective depth of the RC beam with L_{ub}, for the RC beams shown in Figs. 1(a) and (c), $h_0^{pub} = h_0$, where h_0 is the effective depth of perfectly bonded RC beam; for the RC beam shown in Fig. 1(b), h_0^{pub} is conservatively modified as $h_0^{pub} = h_c + d/2$, where d is diameter of exposed tensile steel (Wang and Liu 2009). M'_{cr} is the cracking moment, for the RC beams shown in Fig. 1, $M'_{cr} = f_r bh^2/6$ by assuming a_{cr} to be located out of the edge of the length L_{ub}.

When the flexural crack initiated at location a_{cr}, propagates and reaches the neutral axis, the corresponding location of this critical section a_1 is given as follows by assuming the 45 degrees of the average angle of the tensile cracking

$$a_1 = a_{cr} + h - x_c^v \tag{4}$$

where x_c^v is the depth of compression zone at critical section GG' shown in Fig. 1.

When the tensile crack reaches the neutral axis, the relationship among the moments at the locations a_{cr}, a_1 and the loading point (M_{cr}, M_1 and M_P^v) can be defined as (Park *et al.* 2006, Choi *et al.* 2007)

$$\frac{M_{cr}}{a_{cr}} = \frac{M_1}{a_1} = \frac{M_P^V}{a_v} \tag{5}$$

For beam in Fig. 1, the moment M_1 at critical section a_1 is given as follows

$$M_1 = \int_0^{x_c^v} \sigma(z)dz \cdot b \cdot z_m^v = b \cdot f_c' \cdot x_c^v \cdot [\varepsilon_c^v/\varepsilon_0 - (\varepsilon_c^v/\varepsilon_0)^2/3] \cdot (h_0^{pub} - 0.5\beta_c^v \cdot x_c^v) \tag{6}$$

$$\beta_c^v = \frac{4 - \varepsilon_c^v/\varepsilon_0}{6 - 2\varepsilon_c^v/\varepsilon_0} \tag{7}$$

where ε_c^v is the compressive strain at extreme compression fiber at a_1; β_c^v is stress block factor.

For the RC beams shown in Figs. 1(a) and (b), considering the proposed compatibility condition of deformations of RC beam with partially unbonded length L_{ub} by Wang and Liu (2009) and the horizontal equilibrium condition of forces of the beam, x_c^v at a_1 can be expressed as a function of ε_c^v as follows

$$\varepsilon_s^v = \varepsilon_c^v \cdot \frac{h_0^{pub} - x_c^v}{x_c^v} \cdot \left[1 - \frac{L_{ub} \cdot (L - L_{eq})}{L^2}\right] \tag{8}$$

$$E_s \cdot \varepsilon_s^v \cdot A_s = b \cdot f_c' \cdot x_c^v \cdot [\varepsilon_c^v/\varepsilon_0 - (\varepsilon_c^v/\varepsilon_0)^2/3] \tag{9}$$

where L_{ub} satisfies $0 \le L_{ub} \le L$; L_{eq} is the equivalent plastic region length of corresponding unbonded RC beam, where the whole beam span L of this beam is complete loss of bond; L is the length of the beam span; ε_s^v is the tensile strain of the reinforcements at a_1, $\varepsilon_s^v \le \varepsilon_y$; if $\varepsilon_s^v > \varepsilon_y$, $\varepsilon_s^v = \varepsilon_y$; A_s is the cross section of the longitudinal steel reinforcement. Correspondingly, the moments M_P^V at loading point of the beam with partially unbonded length is also determined by the proposed compatibility condition of deformations and the equilibrium condition of forces

$$\varepsilon_s^P = \varepsilon_c^P \cdot \frac{h_0^{pub} - x_c^P}{x_c^P} \cdot \left[1 - \frac{L_{ub} \cdot (K - L_{eq})}{L^2}\right] \tag{10}$$

$$E_s \cdot \varepsilon_s^P \cdot A_s = b \cdot f_c' \cdot x_c^P \cdot [\varepsilon_c^P/\varepsilon_0 - (\varepsilon_c^P/\varepsilon_0)^2/3] \tag{11}$$

$$M_P^V = \int_0^{x_c^P} \sigma(z)dz \cdot b \cdot z_m^P = b \cdot f_c' \cdot x_c^P \cdot [\varepsilon_c^P/\varepsilon_0 - (\varepsilon_c^P/\varepsilon_0)^2/3] \cdot (h_0^{pub} - 0.5\beta_c^P \cdot x_c^P) \tag{12}$$

$$\beta_c^P = \frac{4 - \varepsilon_c^P/\varepsilon_0}{6 - 2\varepsilon_c^P/\varepsilon_0} \tag{13}$$

where ε_c^P is the compressive concrete strain at extreme compression fiber at loading point; ε_s^P is the tensile strain of the unbonded or exposed reinforcements at loading point, $\varepsilon_s^P \le \varepsilon_y$; if $\varepsilon_s^P > \varepsilon_y$, $\varepsilon_s^P = \varepsilon_y \cdot x_c^P$ is the depth of compression zone at loading point; β_c^P is the stress block factor at loading point.

For the RC beams shown in Fig. 1(c), both the contribution of the bonded steel and the exposed lower unbonded steel are considered. Similar to the RC beams shown in Figs. 1(a) and (b), the x_c^v at a_1 can be given as follows

$$\varepsilon_{sb}^v = \varepsilon_c^v \cdot \frac{h_0^{pub} - x_c^v}{x_c^v} \tag{14}$$

$$\varepsilon_s^v = \varepsilon_c^v \cdot \frac{h_c - x_c^v}{x_c^v} \cdot \left[1 - \frac{L_{ub} \cdot (L - L_{eq})}{L^2}\right] \tag{15}$$

$$E_s \cdot A_s^b \cdot \varepsilon_{sb}^v + E_s \cdot A_s^{ub} \cdot \varepsilon_s^v = b \cdot f_c' \cdot x_c^v \cdot [\varepsilon_c^v/\varepsilon_0 - (\varepsilon_c^v/\varepsilon_0)^2/3] \tag{16}$$

where A_s^b and A_s^{ub} are the areas of the longitudinal bonded and unbonded or exposed steel reinforcement, respectively; ε_{sb}^v and ε_s^v are the strain of the longitudinal bonded and unbonded or exposed steel reinforcement at a_1, respectively, $\varepsilon_{sb}^v \le \varepsilon_y$; if $\varepsilon_{sb}^v > \varepsilon_y$, $\varepsilon_{sb}^v = \varepsilon_y$; $\varepsilon_s^v \le \varepsilon_y$; if $\varepsilon_s^v > \varepsilon_y$, $\varepsilon_s^v = \varepsilon_y$.

Correspondingly, the moments M_P^V at loading point of the beam is given as

$$\varepsilon_{sb}^P = \varepsilon_c^P \cdot \frac{h_0^{pub} - x_c^P}{x_c^P} \tag{17}$$

$$\varepsilon_s^P = \left[1 - \frac{L_{ub} \cdot (L - L_{eq})}{L^2}\right] \cdot \varepsilon_c^P \cdot \frac{h_c - x_c^P}{x_c^P} \tag{18}$$

$$E_s \cdot A_s^b \cdot \varepsilon_{sb}^P + E_s \cdot A_s^{ub} \cdot \varepsilon_s^P = b \cdot f_c' \cdot x_c^P \cdot [\varepsilon_c^P/\varepsilon_0 - (\varepsilon_c^P/\varepsilon_0)^2/3] \tag{19}$$

$$M_P^V = \int_0^{x_c^P} \sigma(z)dz \cdot b \cdot z_m^P = b \cdot f_c' \cdot x_c^P \cdot [\varepsilon_c^P/\varepsilon_0 - (\varepsilon_c^P/\varepsilon_0)^2/3] \cdot (h_0^{pub} - 0.5\beta_c^P \cdot x_c^P) \tag{20}$$

$$\beta_c^P = \frac{4 - \varepsilon_c^P/\varepsilon_0}{6 - 2\varepsilon_c^P/\varepsilon_0} \tag{21}$$

where ε_{sb}^P is the tensile strain of the bonded reinforcements at loading point, $\varepsilon_{sb}^P \le \varepsilon_y$; if $\varepsilon_{sb}^P > \varepsilon_y$, $\varepsilon_{sb}^P = \varepsilon_y$; $\varepsilon_s^P \le \varepsilon_y$; if $\varepsilon_s^P > \varepsilon_y$, $\varepsilon_s^P = \varepsilon_y$.

From Eqs. (3) and (5), the crack initiated location a_{cr} is defined as

$$a_{cr} = \frac{M_{cr}'}{M_P^V/a_v - 0.05\sqrt{f_c'} \cdot b \cdot h_0^{pub}} \tag{22}$$

For the slender beam (shear span ratio $a_v/h_0 > 2.3$) subject to concentrated load, the critical crack

initiated at location a_{cr} propagates to the neutral axis at location a_1 and extends toward the loading point (see Fig. 2(a)). Therefore, the shear capacity of the compression zone must be defined along the inclined failure surface GH in Fig. 2(a). It is difficult to evaluate the allowable shear stresses along the inclined failure surface, however, because the curvature and normal stresses vary along the failure surface. Therefore, for convenience in calculation, the shear capacity of the cross section of GG' was assumed to be identical to that of the inclined failure surface of GH (Park *et al.* 2006, Choi *et al.* 2007). Assuming the shear resistance of a slender beam is mainly provided by the compression zone of the intact concrete (Zhang 1997, Tureyen and Frosch 2003, Park *et al.* 2006, Choi *et al.* 2007), and introducing the average normal stress $\overline{\sigma}(\varepsilon_c^v)$ in the compression zone of the cross section GG' and the size effect factor λ, the minimum shear strength V_c contributed by concrete at location a_1 is defined as (Park *et al.* 2006, Choi *et al.* 2007)

$$V_c = \lambda \cdot b \int_0^{x_c^v} v_u(x)dx \approx \lambda \cdot \sqrt{f_t(f_t + \overline{\sigma}(\varepsilon_c^v))} \cdot b \cdot x_c^v \tag{23}$$

$$\lambda = 1.2 - 0.2\frac{a_v}{h_0} h_0 \geq 0.65 \quad h_0 \text{ in meters} \tag{24}$$

where f_t is the tensile strength of concrete, $f_t = 0.292\sqrt{f_c'}$.

For the beam shown in Fig. 1, due to the compressive strain at extreme compression fiber at a_1 is ε_c^v, the average normal stress $\overline{\sigma}(\varepsilon_c^v)$ of the cross section GG' is given as

$$\overline{\sigma}(\varepsilon_c^v) = f_c' \cdot [\varepsilon_c^v/\varepsilon_0 - (\varepsilon_c^v/\varepsilon_0)^2/3] \tag{25}$$

For the deep beam (shear span ratio $a_v/h_0 \leq 2.3$) subject to concentrated load, the critical crack initiated at location a_{cr} propagates to the neutral axis at location a_1 and combined failure along the inclined tensile cracking GH and compression crushing HJ occurs in the compression zone, see Fig. 2(b). Due to the same reason, the shear capacity of the inclined failure surface of GH was evaluated by the sum of the shear contributions of cross section GG' and HJ (Choi *et al.* 2007). Introducing the average normal stress $\overline{\sigma}(\varepsilon_c^v)$ in the compression zone of the cross section GG' and the size effect factor λ, the minimum shear strength V_c contributed by concrete at location a_1 is defined as (Choi *et al.* 2007)

$$V_c = \lambda \cdot \sqrt{f_t(f_t + \overline{\sigma}(\varepsilon_c^v))} \cdot b \cdot (x_c^v - x_c') + \sqrt{f_c'(f_c' - \overline{\sigma}')} \cdot b \cdot x_c' \tag{26}$$

where $\overline{\sigma}'$ equals the average compressive normal stress developed in the failure surface HJ of compression crushing in the compression zone; x_c' equals the depth of the failure surface HJ of compression crushing, defining as a function of a_v/h_0 (Choi *et al.* 2007)

$$x_c' = (1 - 0.43 \cdot a_v/h_0) \cdot x_c^v \geq 0 \tag{27}$$

For the deep beam in Fig. 1, the average normal stress $\overline{\sigma}(\varepsilon_c^v)$ in Eq. (26) is also given as by Eq. (25). Assuming the average compressive normal stress $\overline{\sigma}'$ in the failure surface HJ to be identical to that developed in the compression zone H'J at the loading point (Choi *et al.* 2007), from Eqs. (5), (6), and (12) or (20), $\overline{\sigma}'$ is defined as a function of ε_c^P or $\overline{\sigma}(\varepsilon_c^v)$ as follows

$$\overline{\sigma}' = f_c' \cdot [\varepsilon_c^P/\varepsilon_0 - (\varepsilon_c^P/\varepsilon_0)^2/3] \tag{28a}$$

$$\overline{\sigma}' = \frac{x_c^v \cdot (h_0^{pub} - 0.5\beta_c^v \cdot x_c^v) \cdot a_v}{x_c^P \cdot (h_0^{pub} - 0.5\beta_c^P \cdot x_c^P) \cdot (a_{cr} + h - x_c^v)} \cdot \overline{\sigma}(\varepsilon_c^v) \tag{28b}$$

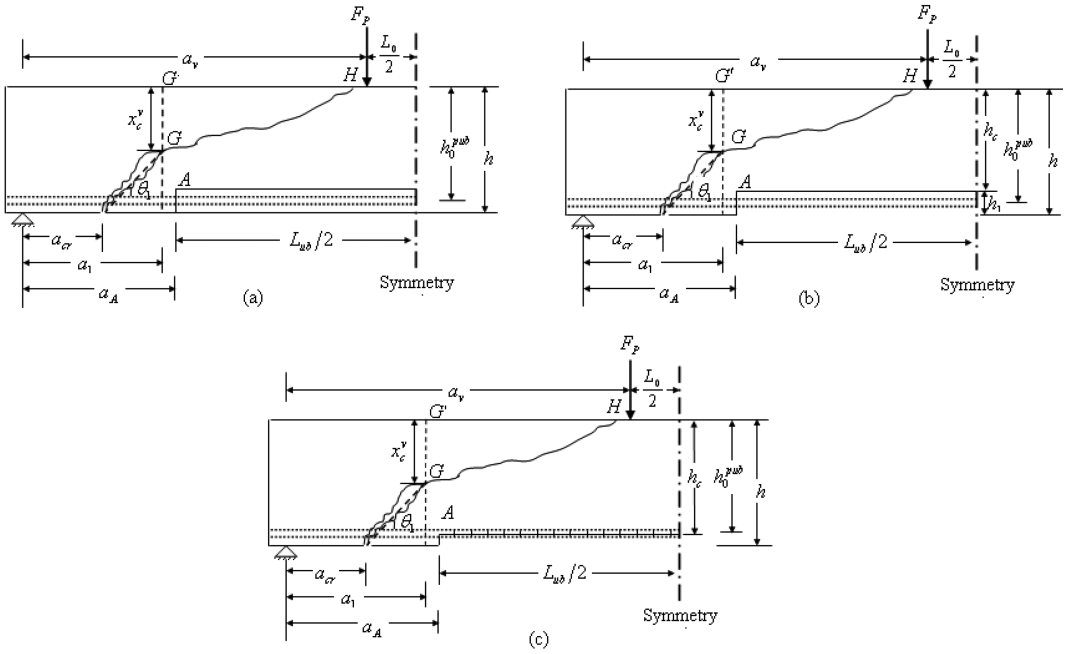

Fig. 1 Scheme of the shear failure for RC beam with partial length L_{ub}: (a) beam with concrete cover and unbonded steel within L_{ub}, (b) beam with whole-exposed steel within L_{ub} and (c) beam with half-exposed lower tensile steel and defective stirrup anchorages within L_{ub}

The shear demand force V_d developing at a cross section of a simply supported beam subjected to concentrated load can be defined as

$$V_d = \frac{M_P^V}{a_v} \tag{29}$$

Then, to determine V_c and a_1 of the beam with L_{ub} in Fig. 1, an arbitrary value of ε_c^P at the loading point is selected. Then, moments M_P^V at loading point is calculated by Eqs. (10)-(13) or Eqs. (17)-(21); and the location a_{cr} is determined by Eq. (22). For an arbitrary value of ε_c^v, the depth x_c^v at a_1 can be determined by Eqs. (8)-(9) or Eqs. (14)-(16). Insert ε_c^v, x_c^v into Eqs. (4)-(7) and the relationship $M_{cr}/a_{cr} = M_1/a_1$ is checked. If this relationship is not satisfied, iterative calculations for new values of ε_c^v are required. Inserting ε_c^v, x_c^v into Eq. (23) or (26), V_c can be determined; inserting ε_c^P and x_c^P into Eq. (29), V_d is calculated. If the calculated shear strength V_c and shear demand force V_d are not identical, iterative calculations for new values of ε_c^P are required. Using the values of ε_c^P corresponding to the time when the shear demand force first reaches the shear strength, the location of the critical section a_1 and the shear strength V_c can be determined (Eq. (23) or (26)).

For the RC beam in Fig. 1, when the stirrups is presented, the shear strength of beam with shear reinforcement is defined as the sum of the shear contributions of concrete and shear reinforcement by neglecting the interaction between the shear mechanism contributed by concrete and the shear mechanism contributed by stirrups

$$V_n^{pub} = V_c + V_s \tag{30}$$

where V_s is the shear strength contributed by stirrups, for the RC beams shown in Figs. 1(a) and (b) with stirrups, V_s is given as follows

For beam with $a_v/h_0>2.3$ $$V_s=\frac{A_{sv}}{b\cdot s_v}\cdot f_{yv}\cdot bh_0^{pub} \tag{31a}$$

For beam with $2\le a_v/h_0\le 2.3$ $$V_s=\frac{A_{sv}}{b\cdot s_v}\cdot f_{yv}\cdot b(h_0^{pub}-2x_c') \tag{31b}$$

For the RC beams with defective stirrup anchorages (Fig. 1(c)), V_s is given as follows

For beam with $a_v/h_0>2.3$ $$V_s=[\eta\beta+(1-\beta)]\cdot\frac{A_{sv}}{b\cdot s_v}\cdot f_{yv}\cdot bh_0^{pub} \tag{32a}$$

For beam with $2\le a_v/h_0\le 2.3$ $$V_s=[\eta\beta+(1-\beta)]\cdot\frac{A_{sv}}{b\cdot s_v}\cdot f_{yv}\cdot b(h_0^{pub}-2x_c') \tag{32b}$$

where β is the proportion of stirrups lacking end anchorages, η is a factor, given as (Regan and Kennedy Reid 2004)

if $(h_0^{pub}-a_s')\ge 2l_{yv}$ $$\eta=1-\frac{l_{yv}}{h_0^{pub}-a_s'} \tag{33a}$$

if $(h_0^{pub}-a_s')<2l_{yv}$ $$\eta=\frac{h_0^{pub}-a_s'}{4l_{yv}} \tag{33b}$$

where a_s' is distance from the extreme compressive fiber to the centroid of the compressive steel; l_{yv} is the bond length of the plain stirrup required to develop yield, given as follows

$$l_{yv}=d_{sv}\cdot\frac{f_{yv}}{4\times 0.78\sqrt{f_{cu}}} \tag{34}$$

For the RC beams shown in Figs. 1(a) and (b), when no stirrups is presented, if the beam fails in inclined shear failure, the corresponding tensile force T_s^v within L_{ub} is given as follows

$$T_s^v=A_s\cdot E_s\cdot\varepsilon_s^P \tag{35a}$$

For the RC beams shown in Figs. 1(a) and (b), when the stirrups is presented, if the beam fails in inclined shear failure, the corresponding tensile force T_s^v within L_{ub} is approximately estimated as follows

$$T_s^v=\frac{V_n^{pub}\cdot a_v}{(h_0^{pub}-0.5\beta_c^P\cdot x_c^P)} \tag{35b}$$

If the tensile force T_s^v determined by Eq. (35) is larger than the yielding tensile force $A_s\cdot f_y$, then let $T_s^v=A_s\cdot f_y$.

For the RC beams shown in Fig. 1(c), due to only the lower tensile steel is half-exposed within L_{ub}, the bond strength within L_{ub} remains resulting in normal strain distribution at the cross section GG'. For the RC beams shown in Figs. 1(a) and (b), however, the normal strain distribution assumption at the cross section GG' should be checked due to the complete elimination of the bond within the partial length L_{ub}. So, the pattern of strains in the concrete body within the partial length L_{ub} is analyzed. Unlike the bond-perfected RC beam, due to the constant tensile stress and force within

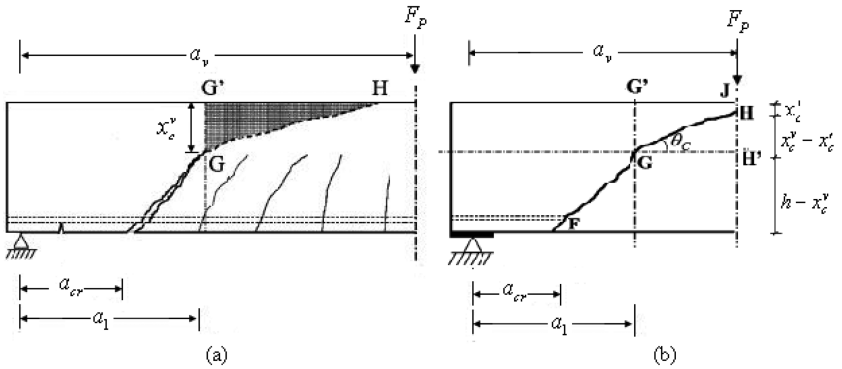

Fig. 2 Shear inclined failure of RC beam with different shear span ratio: (a) tension failure along surface GH for beam with $a_v/h_0 > 2.3$ and (b) combined failure surface of inclined tensile cracking GH and compression crushing HJ in the compression zone for beam with $a_v/h_0 \leq 2.3$ (Choi *et al.* 2007)

L_{ub}, three different strain patterns may present: (1) the normal strain distribution in the concrete body-the concrete is subjected to compressive stress in the top part and subjected to tensile stress in the bottom part of the beam; (2) the whole concrete body is subjected to compressive stress and (3) the inverse strain distribution in the concrete body. The scheme of the pattern of strains in the concrete body within the partial length L_{ub} is shown in Fig. 3. Within the partial length L_{ub}, the thrust line is a straight diagonal line resulting from the loss of bond (Kani 1964, Park and Paulay 1975). Outside the unbonded length, the tensile force of the steel uniformly distributed along the reinforcing bars, as indicated by the equal ΔT force resulting from the bond stress between two materials.

The positions of a_{tri} and a_{tri}^T shown in Fig. 3 are approximately determined as follow
for Fig. 3(a)

$$a_{tri} = \frac{T_s \cdot (h/3 - a_s)}{F_P} \qquad a_{tri}^T = \frac{T_s \cdot (2h/3 - a_s)}{F_P} \tag{36}$$

for Fig. 3(b)

$$a_{tri} = \frac{T_s \cdot [(h - h_1)/3 + (h_1 - a_s)]}{F_P} \qquad a_{tri}^T = \frac{T_s \cdot [2(h - h_1)/3 + (h_1 - a_s)]}{F_P} \tag{37}$$

where a_s is the distance from the extreme tensile fiber to the centroid of the tensile steel.

Corresponding to the strain pattern in the concrete body within L_{ub} shown in Fig. 3, the specified conditions that cause shear failure mode are discussed. For the shear failure line shown in Figs. 1(a) and (b), due to the different strain distribution in the concrete body near the end of the partial length in Fig. 3 and the normal strain distribution assumption at the cross section GG', shear failure can occur if the critical section a_1 locates outside the partial length, i.e., $a_1 < a_A$. For the RC beam with stirrups, although the location of the critical section and the shear strength of concrete of a beam with stirrups are different from those of a beam without stirrups (Choi *et al.* 2007), the influence of the stirrups on the location of the critical section is not considered and the interaction between the concrete and shear reinforcement is neglected.

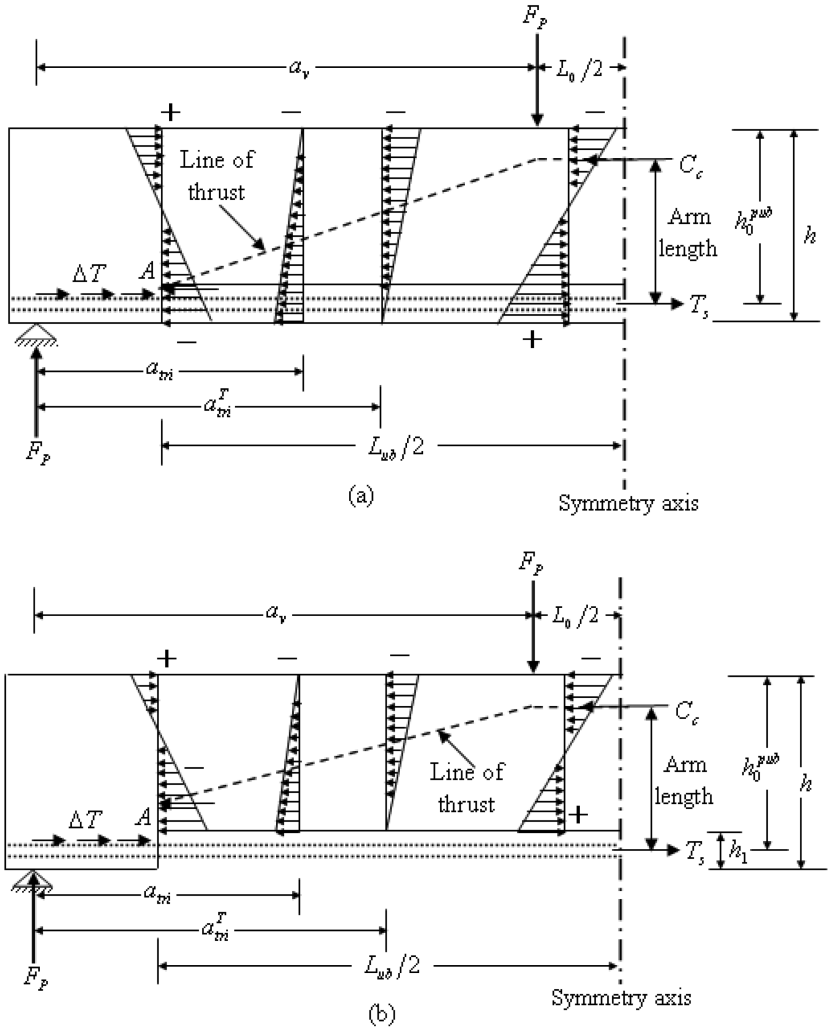

Fig. 3 Scheme of the pattern of strains in the concrete body within the partial length L_{ub}: (a) with concrete cover and (b) without concrete cover and with exposed steel

4. Numerical procedure for shear strength of the RC beam with L_{ub}

According to the proposed methodology in the above section, the analytical procedure for shear strength V_n^{pub} of the RC beam with L_{ub} is shown in Fig. 4. In Fig. 4, for beams shown in Figs. 1(a) and (b), the specified condition $a_1 < a_A$ is considered in the numerical procedure.

5. Examination of model accuracy

In the test studies of Kim and White (1999) and Yu (2005), tests were conducted on simply supported RC beams with two-point symmetrical loads, where complete loss of bond over partial

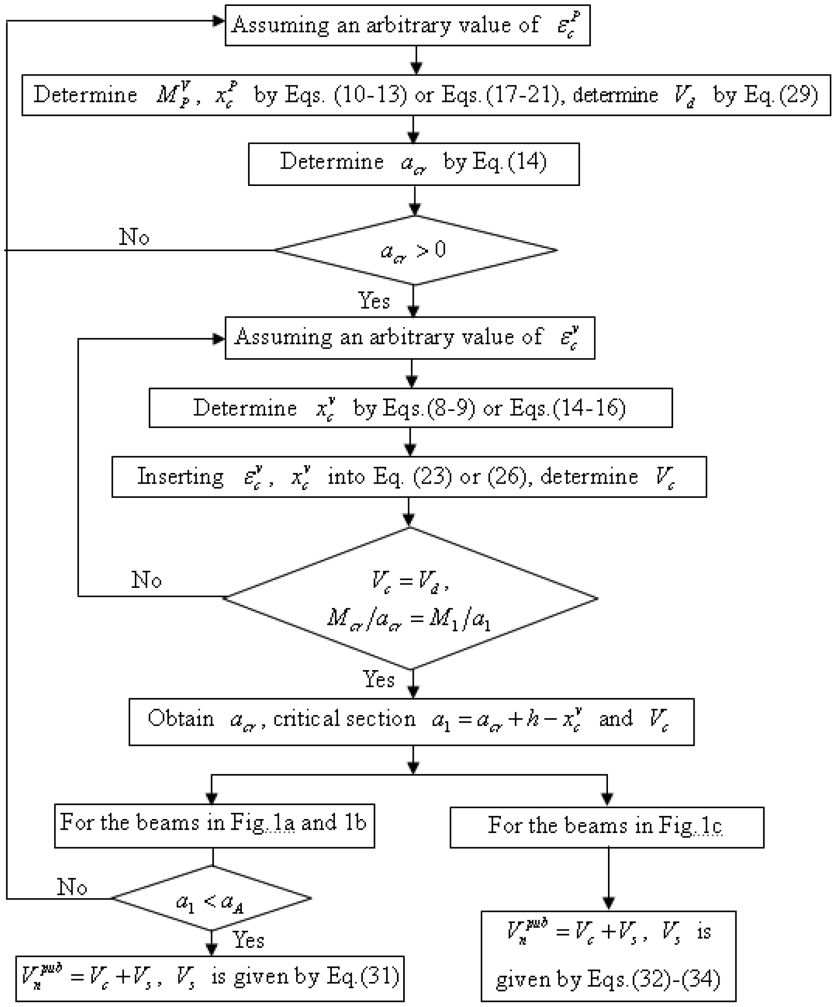

Fig. 4 Analytical procedure for shear strength V_n^{pub} of the RC beam with partial length L_{ub}

length symmetrically arranged about the mid-span were presented in some test specimens. In the test of Kim and White (1999), all RC beams had concrete cover and unbonded steel within L_{ub}; In the RC beams of Yu (2005), all tensile bars were exposed. In the test studies of Regan and Kennedy Reid (2004), beam specimens were simply supported and subjected to central concentrated loads. In the four beams 9, 10, 13 and 14, the lower main bars were half-exposed and 67% of the stirrups lacked end anchorages within L_{ub}.

Based on the proposed models, shear strength of the RC beams with continuously partial length L_{ub} are calculated and compared with the corresponding test results, see Tables 1-3. In Table 1, test beams were rectangular concrete beams, each 127 mm × 229 mm, with two 15.9-mm- diameter high-strength bars as tension reinforcements. The effective depth was 191 mm. The 15.9 mm longitudinal reinforcement had actual f_y = 461 MPa. In Table 2, test beams were also rectangular beams, each 180 mm × 300 mm, with three 20-mm-diameter high-strength bars as tension bars and two 10 mm-diameter plain bars as stirrup-holders. The 20 mm longitudinal reinforcement had actual f_y = 390

Table 1 Comparison with experimental results of Kim and White (1999)

Specimen	L_{ub} (mm)	f_c' (MPa)	Test results (kN)		Predicted load P_{cal}^{pub} (kN)	$\frac{P_{exp}^{pub}}{P_{cal}^{pub}}$
			$V_{n,cr}^{pub}$	Ultimate load P_{exp}^{pub}		
3CNB	0	37.7	57.8	58.7	71.5	0.808
3UBB1	1244	27.1	–	96.5	102.12	0.945
4CNB	0	34.9	60.5	60.5	67.38	0.898
4UBB1	1626	28.4	–	76.1	77.28	0.985
Mean value 0.909 Standard deviation 0.076						

Table 2 Comparison with experimental results of Yu (2005)

Specimen	Details of the test RC beam				Experimental shear strength $V_{n,exp}^{pub}$ (kN)	Predicted shear strength $V_{n,cal}^{pub}$ (kN)	$\frac{V_{n,exp}^{pub}}{V_{n,cal}^{pub}}$
	b (mm)	h_0 (mm)	L_{ub} (mm)	f_{cu} (MPa)			
JL-0	180	275	0	24.50	227	228.92	0.992
JL-1	180	275	400	26.44	199	212.92	0.935
JL-3	182	275	800	23.06	233	203.70	1.144
JL-5	183	278	1600	24.22	190	197.94	0.960
Mean value 1.008 Standard deviation 0.094							

Table 3 Comparison with experimental results of Regan and Kennedy Reid (2004)

Beam No.	Details of the test RC beam							Experimental shear strength $V_{n,exp}^{pub}$ (kN)	Predicted shear strength $V_{n,cal}^{pub}$ (kN)	$\frac{V_{n,exp}^{pub}}{V_{n,cal}^{pub}}$
	h_0 (mm)	A_s (mm^2)	A_{sv} (mm^2)	L_{ub} (mm)	f_y (MPa)	f_{yv} (MPa)	f_{cu} (MPa)			
7	340	4Φ25	ϕ8@150	0	475	350	47.3	207	181.21	1.142
9	340	4Φ25	ϕ8@150	2400	475	350	45.0	165	140.51	1.174
10	340	4Φ25	ϕ8@150	2400	475	350	49.7	140	145.14	0.965
11	200	4Φ20	ϕ6@75	0	500	330	47.5	126	122.83	1.025
13	200	4Φ20	ϕ6@75	1400	500	330	50.7	90	93.53	0.962
14	200	4Φ20	ϕ6@75	1400	500	330	50.7	96	93.53	1.026
Mean value 1.049 Standard deviation 0.089										

MPa. The shear reinforcements consist of 6.5 mm-diameter plain stirrups at 120 mm on center in the shear span, where 6.5 mm-diameter plain stirrup had yield strength of 280 MPa. In Table 3, all test beams were rectangular concrete beams and have beam width 150 mm. Beams 7, 9 and 10 were 150 mm × 400 mm in section and 3 m long. They were simply supported on spans of 2.5 m; while beams 11, 13 and 14 were 150 mm × 250 mm in section and 2 m long. They were tested with central loads on spans of 1.5 m.

The accuracy of the proposed models is examined, at the bottom of the Tables 1-3, by means of the experimental-to-calculated ratio $P_{exp}^{pub}/P_{cal}^{pub}$ or $V_{n,exp}^{pub}/V_{n,cal}^{pub}$ mean value and standard deviation, where P_{exp}^{pub} and P_{cal}^{pub} are the experimental and calculated ultimate load of the RC beam with L_{ub},

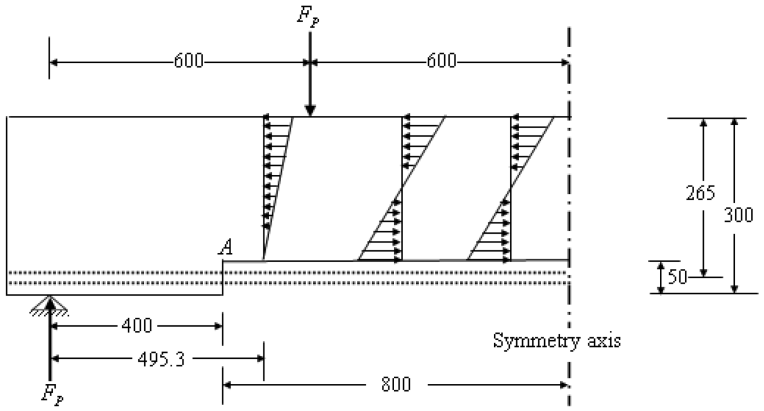

Fig. 5 Strain distributions in the concrete body beam JL-5 of Yu (2005) (Dimension: mm)

respectively; $V_{n,exp}^{pub}$ and $V_{n,cal}^{pub}$ are the experimental and calculated shear strength of the RC beam with L_{ub}, respectively; $V_{n,cr}^{pub}$ is the experimental shear cracking strength. It can be seen from the Tables that the proposed model provided good predictions.

For the beams 3UBB1 and 4UBB1 in the test of Kim and White (1999), where over 80% shear span is unbonded, due to the existence of the unbonded length, the critical inclined crack a_1 can not form within the shear span, avoiding the typical diagonal shear failure of the corresponding perfectly bonded beam 3CNB and 4CNB. So, both beams fail in typical flexure failure-concrete crushing at constant moment zone after the yielding of the tensile bars.

For the beams JL-1, JL-3 and JL-5 in the test of Yu (2005), where the maximum unbonded length within shear span is lower than 30%, due to the long distance of a_A and enough flexural tensile bars, the critical inclined crack a_1 is always located within a_A and the beam fails in shear failure, just like the shear failure of bonded beam JL-0. At the ultimate state, the tensile force T_s^v within L_{ub} and the corresponding shear capacity are taken into Eqs. (36) and (37) to determine the pattern of strains in the concrete body within the partial length L_{ub}. Since the constant moment zone of test specimens in Yu (2005) is 1200 mm, only the strain distributions in the concrete body within the partial length of beam JL-5 is considered in Fig. 5. It can be seen from Fig. 5 that, due to the long length of a_A, the whole concrete body is subjected to compressive stress between the loading point and a_A.

6. Discussion

6.1 Influence of the partially unbonded length on the shear capacity of the RC beam

For the corresponding perfectly bonded RC beam fails in shear failure, the influence of the partially unbonded length on the shear capacity of the RC beam is studied. Numerical simulation results are obtained from a beam of identical cross section to beam 4UBB1 of Kim and White (1999), with the same other parameters except for variable L_{ub} and a_A. The effect of the length L_{ub} on the load capacity of the RC beam with partially unbonded length is shown in Fig. 6, where the relative shear capacity ratio describes the ratio of shear capacity of beam with L_{ub} to the shear

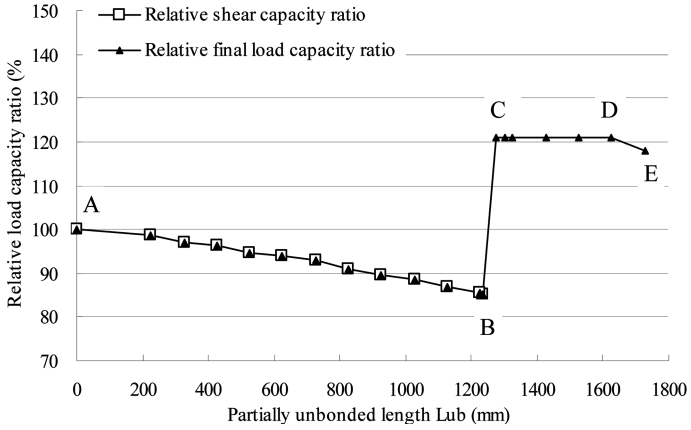

Fig. 6 Effect of the length L_{ub} on the load capacity of the RC beam, where the corresponding perfectly bonded RC beam fails in shear failure

capacity of perfectly bonded beam; while the relative final load capacity ratio describes the ratio of final load capacity of beam with L_{ub} to the final load capacity of perfectly bonded beam. For perfectly bonded beam failing in shear, the final load capacity of the beam equals to its shear capacity. In Fig. 6, in stage AB, due to the comparative shorter partially unbonded length, the critical inclined crack can form within the shear span resulting in the same failure mode as the perfectly bonded beam; with the increase of the partial length, the critical inclined crack can not form within the shear span and the original shear failure is avoided. Not only ductile performance of the beam is presented resulting from the yielding of the tensile steel bars (stage CD in Fig. 6), the load capacity is also greatly increased, as pointed out by Cairns (1995) and Kim and White (1999). With the further increase of the partial length, the tensile steel can not yield and the load capacity begins to decrease (stage DE in Fig. 6).

6.2 Influence of the percentage of the stirrups lacked end anchorages on the shear capacity of the RC beam

For the corresponding perfectly bonded RC beam fails in shear failure, the influence of the percentage of the stirrups lacked end anchorages on the shear capacity of the RC beam is studied. Numerical simulation results are obtained from a beam of identical cross section to beam 13 of Regan and Kennedy Reid (2004), with the same other parameters except for variable β in Eq. (32). The distributions of the stirrups in beam 13 of Regan and Kennedy Reid (2004) and the identical beams with different β are shown in Fig. 7. The effect of the percentage of the stirrups lacked end anchorages on the shear capacity of the RC beam is shown in Fig. 8, where the relative shear capacity ratio describes the ratio of shear capacity of beam with β within length L_{ub} to the shear capacity of the corresponding perfectly bonded beam. It can be seen from Fig. 8 that the loss of the shear strength with different β within length L_{ub} compared to that of the perfectly bonded beam failed in shear increased with the increase of the percentage of the stirrups lacked end anchorages. For RC beam with perfectly stirrups and half-exposed tensile reinforcements (Fig. 7(c)), the loss of the shear strength compared to that of the perfectly bonded beam is 11.8%; while for beam with 67% stirrups lacked end anchorages and half-exposed tensile reinforcements within the same partial

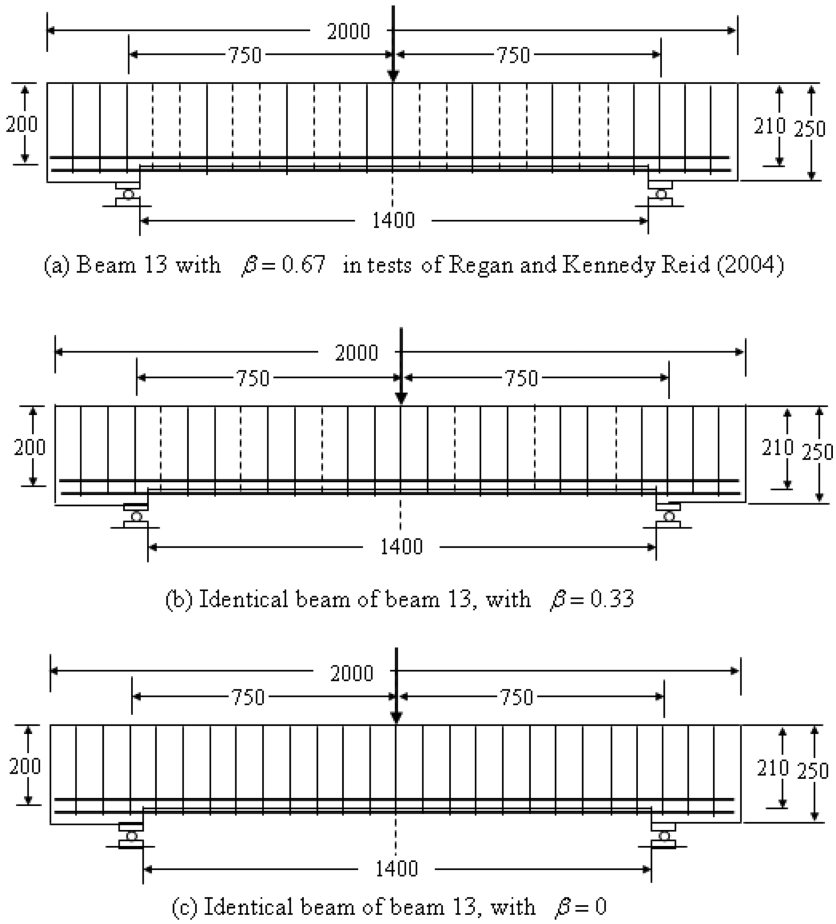

Fig. 7 The distributions of the stirrups in beam 13 of Regan and Kennedy Reid (2004) and the identical beam with different β

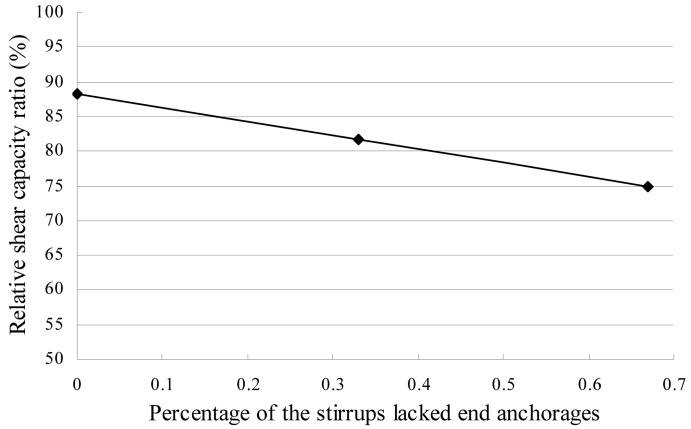

Fig. 8 Influence of the percentage of the stirrups lacked end anchorages β on the load capacity of the RC beam, where the corresponding perfectly bonded RC beam fails in shear failure

length (Fig. 7(a)), this loss of the shear strength is 25%. Thus, 67% stirrups lacked end anchorages results in nearly 14% loss of shear strength of the beam, making a comparatively big contribution to the shear resistances loss of reinforced concrete beams.

7. Conclusions

Considering the possible position of the critical inclined crack, shear strength of the RC beam with unbonded or exposed tensile steel and/or defective stirrup anchorages is theoretically predicted. The accuracy of the proposed model is examined by comparing the model's predictions with the results of experimental study carried out by Kim and White (1999), Yu (2005) and Regan and Kennedy Reid (2004). Good agreement is shown between the predicted results and the corresponding test results. Then, the effects of the partially unbonded length and the percentage of the stirrups lacked end anchorages on the shear capacity of the RC beam are discussed.

For a given RC beam with given unbonded length, the possibility of the shear failure is mainly related to the form of the critical inclined crack within shear span. If the partially unbonded length is long resulting in no form of the critical inclined crack within the shear span, the original typical shear failure of the normal bonded RC beam may be avoided. As a result, failure mode of the beam with partially unbonded length may change into typical flexure failure and the corresponding load capacity increases compared with the normal bonded RC beam; if the partially unbonded length is small or located in the constant moment zone resulting in the form of the critical inclined crack within the shear span, the similar shear failure mode may be presented as the normal bonded RC beam. In addition, the load capacity of the RC beam with partially unbonded length decreases with the increase of the partial length.

For the beam with half-exposed tensile reinforcements and stirrups lacked end anchorages within given partial length, the shear strength of the beam is influenced by both the exposed length of the tensile reinforcements and the stirrups lacked end anchorages. The loss of the shear strength with different percentage of the stirrups lacked end anchorages within given partial length compared to that of the perfectly bonded beam increased with the increase of the percentage of the stirrups lacked end anchorages.

It should be pointed out that, due to neglecting the effect of the bond strength between the reinforcing bar and the surrounding concrete within the partial length, the shear strength of the RC beam with partially unbonded length may be different from that of the RC beam with bond strength within the same corroded length. For low and moderate corrosion level of the reinforcing bars within the partial length resulting in bond reduction between the corroded steel and concrete, the critical inclined crack can still form within shear span and similar shear failure mode may be presented as the normal bonded RC beam. Only if the corrosion level of the reinforcing bars within the partial length is very high resulting in complete loss of bond strength between the corroded steel and concrete, the methodology proposed in the present paper can be used to predict the shear capacity of the RC beam with partially corroded length, just considering the corrosion-induced damage of the longitudinal tensile bars and the contacted stirrups.

In addition, the proposed model tends to provide larger values of capacity than experimental results in some cases (see Tables 1 and 2). The main reasons of this trend may result from: (1) the complex of the shear mechanism and the difficulty in exact prediction of the shear strength of the bond-perfect RC beam. Choi and Park (2007) verified their proposed shear strength model of Choi

et al. (2007) by using considerable experimental results published in literature. For RC beam without shear reinforcement, the mean value of the ratios (in the range of 0.8~2.6) of the test results to the predicted shear strength of 400 slender and 177 deep beams was 0.99, with a standard deviation of 0.14; for RC beam with shear reinforcement, the mean value of the ratios (in the range of 0.6~1.8) of the test results to the predicted shear strength of 251 slender and 282 deep beams was 0.98, with a standard deviation of 0.15 (Choi and Park 2007). The discrepancy between the test results and the proposed shear model is always presented and (2) the assumption of fully yielding of the stirrups across inclined tensile cracks in Eqs. (31) and (32). In fact, due to the high shear stress and the effect of coexisting inclined tensile cracking, the concrete of the inclined compression struts may be early crushed and govern the failure mechanism of the concrete beams. So, there exists a upper limit of the contribution of shear reinforcement V_s in Eq. (30). Test results of Yu (2005) also indicated that, at the failure of the test specimens, for the stirrups sequentially located from the loading point to the support, only the second and fourth stirrups yielded in specimens JL-1 while no stirrups yielded in specimens JL-5. Larger predicted shear strength of JL-1 and JL-5 was presented in Table 2. Thus, further research should be focused on: (1) the development of more accurate shear strength predicted model of the bond-perfect RC beam and (2) the consideration of the interaction between the shear mechanism contributed by concrete and the shear mechanism contributed by stirrups in RC beam with partially unbonded length L_{ub} shown in Fig. 1.

The present evaluation approach is a primary step forward to the further study, making it possible to predict the shear capacity of corroded RC beams in the field situations, as required by the assessment of safety in existing deteriorated structures. Compared to the RC beam with unbonded or exposed tensile steel reinforcements and/or defective stirrup anchorages, bond strength between the corroded steel and surrounding concrete is changed with the corrosion level. The corrosion-induced factors, such as the possible reduction in bond strength between the corroded steel and surrounding concrete, the corrosion-damaged longitudinal tensile bars and the contacted stirrups, the longitudinal cracking and the possible ruptured stirrups within shear span should be considered in the further study on the shear capacity of corroded RC beams.

Acknowledgments

The authors gratefully acknowledge the support provided by the National Natural Science Foundation of China (No. 50508020 and No. 51178266).

References

Azam, R. (2010), *Behaviour of shear critical RC beams with corroded longitudinal steel reinforcement*, MSc thesis, Applied Science in Civil Engineering, University of Waterloo, Waterloo, Ontario, Canada.

Cairns, J. (1995), "Strength in shear of concrete beams with exposed reinforcement", *P. I. Civil Eng.-Struct. B.*, **110**(2), 176-185.

Castel, A., Francois, R. and Arliguie, G. (2000), "Mechanical behaviour of corroded reinforced concrete beams Part 1: experimental study of corroded beams", *Mater. Struct.*, **33**(9), 539-544.

Choi, K.K. and Park, H.G. (2007), "Unified shear strength model for reinforced concrete beams-Part II: verification and simplified method", *ACI Struct. J.*, **104**(2), 153-161.

Choi, K.K., Park, H.G. and Wight, J.K. (2007), "Unified shear strength model for reinforced concrete beams-Part

I: Development", *ACI Struct. J.*, **104**(2), 142-152.
Collins, M.P. and Mitchell, D. (1987), *Prestressed concrete basics*, Canadian Prestressed Concrete Institute (CPCI), Ottawa, Ontario, Canada.
Du, Y.G., Clark, L.A. and Chan Andrew, H.C. (2007), "Impact of reinforcement corrosion on ductile behavior of reinforced concrete beams", *ACI Struct. J.*, **104**(3), 285-293.
EI Maaddawy, T., Soudki, K. and Topper, T. (2005), "Long-term performance of corrosion-damaged reinforced concrete beams", *ACI Struct. J.*, **102**(5), 649-656.
Higgins, C. and Farrow III, W.C. (2006), "Tests of reinforced concrete beams with corrosion-damaged stirrups", *ACI Struct. J.*, **103**(1), 133-141.
Jeppsson, J. and Thelandersson, S. (2003), "Behavior of reinforced concrete beams with loss of bond at longitudinal reinforcement", *J. Struct. Eng.-ASCE*, **129**(10), 1376-1383.
Kani, G.N. (1964), "The riddle of shear failure and its solution", *J. Am. Concrete, Inst.*, **61**(4), 441-466.
Kim, W. and White, R.N. (1999), "Shear-critical cracking in slender reinforced concrete beams", *ACI Struct. J.*, **96**(5), 757-765.
Malumbela, G., Moyo, P. and Alexander, M. (2009), "Behaviour of RC beams corroded under sustained service loads", *Constr. Build. Mater.*, **23**(11), 3346-3351.
Park, H.G., Choi, K.K. and Wight, J.K. (2006), "Strain-based shear strength model for slender beams without web reinforcement", *ACI Struct. J.*, **103**(6), 783-793.
Park, R. and Paulay, T. (1975), *Reinforced concrete structures*, John Wiley & Sons, New York.
Regan, P.E. and Kennedy, Reid I.L. (2004), "Shear strength of RC beams with defective stirrup anchorages", *Mag. Concrete Res.*, **56**(3), 159-166.
Suffern, C., El-Sayed, A. and Soudki, K. (2010), "Shear strength of disturbed regions with corroded stirrups in reinforced concrete beams", *Can. J. Civil Eng.*, **37**(8), 1045-1056.
Toogoenthong, K. and Maekawa, K. (2004a), "Interaction of pre-induced damages along main reinforcement and diagonal shear in RC members", *J. Adv. Concrete Tech.*, **2**(3), 431-443.
Toogoenthong, K. and Maekawa, K. (2004b), "Shear capacity of damaged RC beam with partial longitudinal cracks in space", *Proc. Jpn. Concrete Inst.*, **26**(2), 385-390.
Torres-Acosta, A.A., Fabela-Gallegos, M.J., Muñoz-Noval, A., Vázquez-Vega, D., Hernandez-Jimenez, J.R. and Martínez-Madrid, M. (2004), "Influence of corrosion on the structural stiffness of reinforced concrete beams", *Corrosion*, **60**(9), 862-872.
Tureyen, A.K. and Frosch, R.J. (2003), "Concrete shear strength: Another perspective", *ACI Struct. J.*, **100**(5), 609-615.
Vidal, T., Castel, A. and Francois, R. (2007), "Corrosion process and structural performance of a 17 year old reinforced concrete beam stored in chloride environment", *Cement Concrete Res.*, **37**(11), 1551-1561.
Wang, X.H. and Liang, F.Y. (2008), "Performance of RC columns with partial length corrosion", *Nucl. Eng. Des.*, **238**(12), 3194-3202.
Wang, X.H., Gao, X.H., Li, B. and Deng, B.R. (2011), "Effect of bond and corrosion within partial length on shear behaviour and load capacity of RC beam", *Constr. Build. Mater.*, **25**(4), 1812-1823.
Wang, X.H. and Liu, X.L. (2009), "Predicting the flexural capacity of RC beam with partially unbonded steel reinforcement", *Comput. Concrete*, **6**(3), 235-252.
Yu, F.J. (2005), *Experimental study and analysis on the diagonal shear property of corroded reinforced concrete beam*, MSc thesis, College of Civil Engineering, Hohai University, P. R. China.
Zhang, J.P. (1997), "Diagonal cracking and shear strength of reinforced concrete beams", *Mag. Concrete Res.*, **49**(178), 55-65.

CC

Notation

A_s	cross section area of tensile steel
A_{sv}	cross section area of the stirrups
A_s^b	areas of the longitudinal bonded steel reinforcement
A_s^{ub}	areas of the longitudinal unbonded or exposed steel reinforcement
a_A	distance between the support and the extra edge of the partial length
a_{cr}	location of crack initiation at critical section
a_s	distance from the extreme tensile fiber to the centroid of the tensile steel
a_s'	distance from the extreme compressive fiber to the centroid of the compressive steel
a_v	shear span of the RC beam
a_1	critical inclined crack section
b	beam width of rectangular cross section
d, d_{sv}	diameter of tensile steel and stirrups, respectively
E_c	Young's modulus of concrete
E_s	Young's modulus of tensile steel reinforcement
f_c'	cylinder compressive strength of concrete
f_{cu}	cube compressive strength of concrete
f_r	modulus of rupture of concrete, $f_r = 0.625\sqrt{f_c'}$
f_t	tensile strength of concrete, $f_t = 0.292\sqrt{f_c'}$
f_y	yield strength of the tensile steel reinforcement
f_{yv}	yielding strength of the stirrups
$g(L_{ub})$	interpolating function of partial unbonded or exposed length L_{ub}
h_0	effective depth of perfectly bonded RC beam
h_0^{pub}	effective depth of RC beam with L_{ub}
h_c	depth of concrete where reinforcements is fully exposed or half-exposed
L	length of the beam span
L_{eq}	equivalent plastic region length of corresponding unbonded RC beam, where the whole beam span L of the beam is complete loss of bond
L_{ub}	unbonded or exposed length symmetrically arranged about the mid-span of the beam
l_{yv}	bond length of the plain stirrup required to develop yield
M_{cr}	flexural moment at a_{cr}
M_P^V	flexural moments at loading point
M_1	flexural moments at critical section a_1
s_v	space of the stirrups
T_s^v	tensile force of steel within L_{ub}
V_c	shear strength contributed by concrete for RC beam with L_{ub}
V_d	shear demand force of the RC beam with L_{ub}
V_n^{pub}	shear strength of the RC beam with L_{ub}
$V_{n,cal}^{pub}$	calculated shear strength of the RC beam with L_{ub}
$V_{n,exp}^{pub}$	experimental shear strength of the RC beam with L_{ub}

$V_{n,cr}^{pub}$ experimental shear cracking strength
V_s shear strength contributed by stirrups for RC beam with L_{ub}
x_c^P depth of compression zone at loading point
x_c^v depth of compression zone at critical section a_1
x_c' depth of the shear failure surface of compression crushing
z_m^P distance from the extreme compressive fiber to the centroid of the tensile steel at loading point of the beam
z_m^v distance from the extreme compressive fiber to the centroid of the tensile steel at critical section a_1
β percentage of the stirrups lacked end anchorages in the beam
β_c^v, β_c^P stress block factor
ε_{cu} ultimate strain of concrete in compression
ε_c^P compressive concrete strain at extreme compression fiber at loading point
ε_c^v concrete compressive strain at extreme compression fiber at a_1
ε_s^P tensile strain of the unbonded or exposed reinforcements at loading point
ε_{sb}^P tensile strain of the bonded reinforcements at loading point
ε_s^v tensile strain of the reinforcements at a_1
ε_y yield strain of steel reinforcement
λ size effect factor
$\overline{\sigma}(\varepsilon_c^v)$ average normal stress in the compression zone of the section a_1
$\overline{\sigma}'$ average compressive normal stress developed in the shear failure surface of compression crushing in the compression zone